nature chemistry

ARTICLES

PUBLISHED ONLINE: 20 MAY 2012 | DOI: 10.1038/NCHEM.1351

# Biosynthesis of the tunicamycin antibiotics proceeds via unique exo-glycal intermediates

Filip J. Wyszynski[1†], Seung Seo Lee[1†], Tomoaki Yabe[1], Hua Wang[1], Juan Pablo Gomez-Escribano[2], Mervyn J. Bibb[2], Soo Jae Lee[3], Gideon J. Davies[4] and Benjamin G. Davis[1*]

**The tunicamycins are archetypal nucleoside antibiotics targeting bacterial peptidoglycan biosynthesis and eukaryotic protein *N*-glycosylation. Understanding the biosynthesis of their unusual carbon framework may lead to variants with improved selectivity. Here, we demonstrate *in vitro* recapitulation of key sugar-manipulating enzymes from this pathway. TunA is found to exhibit unusual regioselectivity in the reduction of a key α,β-unsaturated ketone. The product of this reaction is shown to be the preferred substrate for TunF—an epimerase that converts the glucose derivative to a galactose. In *Streptomyces* strains in which another gene (*tunB*) is deleted, the biosynthesis is shown to stall at this exo-glycal product. These investigations confirm the combined TunA/F activity and delineate the ordering of events in the metabolic pathway. This is the first time these surprising exo-glycal intermediates have been seen in biology. They suggest that construction of the aminodialdose core of tunicamycin exploits their enol ether motif in a mode of C–C bond formation not previously observed in nature, to create an 11-carbon chain.**

The tunicamycins are fatty acyl nucleoside antibiotics with potent inhibitory activity towards bacterial cell wall biosynthesis and eukaryotic protein *N*-glycosylation[1–3]. They are produced by *Streptomyces lysosuperificus* and *chartreusis* strains[4,5], and their structures comprise a unique 11-carbon core (tunicamine) decorated with uracil, *N*-acetylglucosamine (GlcNAc) and variable fatty acyl moieties (Fig. 1a)[6,7]. Several other natural products share the same carbohydrate core: streptovirudins[8], corynetoxins[9], MM19290[10], mycospocidin[11] and antibiotic 24010[12]. The biosynthetic pathways to this core are all unknown.

Tunicamycins were the first compounds found to specifically inhibit the formation of peptidoglycan precursor lipid I (targeting enzyme MraY) during bacterial cell wall biosynthesis[1,13], a mode of action orthogonal to existing antibiotics[1,14,15]. These antibiotics also inhibit eukaryotic *N*-linked glycoprotein synthesis at the first committed step[2]. Although this results in cytotoxicity to mammalian cells and currently precludes clinical use, it renders tunicamycin a crucial tool in glycobiology[16].

Synthetic studies towards tunicamycins have been published[17–20], including two total syntheses[21,22], but biosynthetic investigations have been limited[23]. Recent identification of the biosynthetic gene cluster and the proposal of a possible metabolic pathway, however, have opened the door to more detailed investigations[24–26]. A deeper understanding of the enzymatic processes involved may allow this unique natural product scaffold to be readily altered. New analogues could be more selective inhibitors of MraY, as well as rationally designed inhibitors of other enzymes.

The biogenesis of the undecose tunicamine core has been predicted[23–26] to involve some form of unusual monosaccharide tail-to-tail C–C coupling (Fig. 1b). Although associated genes have been suggested[24], the actual activity of the gene products and precise ordering of the transformations remain unknown. Here, we show how two enzymes act together at the first committed stages. TunA is shown to have a previously unreported activity in biology as a 5,6-dehydratase, and kinetic analyses and structure provide insights into this novel, unique selectivity. TunF is found to act as a sugar-4-epimerase with unusual substrate tolerance, which helps to delineate pathway ordering. A revised pathway is proposed, involving conjugation of an exo-glycal (the first invoked in any natural pathway) with a suitable uridine derivative.

## Results

**Bioinformatic mining of the *tun* gene cluster.** Within the biosynthetic pathway deduced from the *S. chartreusis tun* gene cluster[24], putative gene products TunA and TunF were suggested to participate in the early construction of the tunicamine subunit (Fig. 1b). Sequence homology comparison and alignment (Supplementary Figs S1 and S2) revealed that TunA was similar to NAD-dependent hexose epimerases and dehydratases from a variety of sources. This suggested TunA to be a member of the short-chain dehydrogenase/reductase (SDR) family. The three closest homologues (identities 27–32%) with Protein Data Bank (PDB)[27] entries are well-characterized 4,6-dehydratases that operate on a substrate very different to that in the tunicamycin pathway, deoxythymidine-diphosphate glucose (dTDP-Glc): DesIV from *Streptomyces venezuelae*, RmlB from *Salmonella enterica* and RmlB from *Streptococcus suis*[28,29]. Multiple sequence alignments suggest mechanistically important amino-acid residues (Supplementary Fig. S1). Importantly, the putative TunA sequence has key conserved motifs for nucleotide binding (TGxxGxxG near N-terminus) and a signature TYK catalytic triad (Thr119, Tyr143, Lys147). In other enzymes, TYK, together with cofactor $NAD^+$, performs the initial oxidation of the 4-OH of hexose substrates[29].

The TunF sequence showed similarity (28–29%) with two of the best characterized NAD-dependent hexose epimerases: WbpP from *Pseudomonas aeruginosa* and WbgU from *Plesiomonas shigelloides*[30,31]. This led to early predictions as a UDP-GlcNAc 4-epimerase and suggested it as the first committed pathway enzyme.

[1]Chemistry Research Laboratory, University of Oxford, 12 Mansfield Road, Oxford OX1 3TA, UK, [2]Department of Molecular Microbiology, John Innes Centre, Norwich Research Park, Norwich NR4 7UH, UK, [3]College of Pharmacy, Chungbuk National University, Gaeshin-dong, Heungduk-gu, Cheongju, Chungbuk, Korea, [4]Department of Chemistry, The University of York, Heslington, York YO10 5DD, UK; [†]These authors contributed equally to this work. *e-mail: ben.davis@chem.ox.ac.uk.

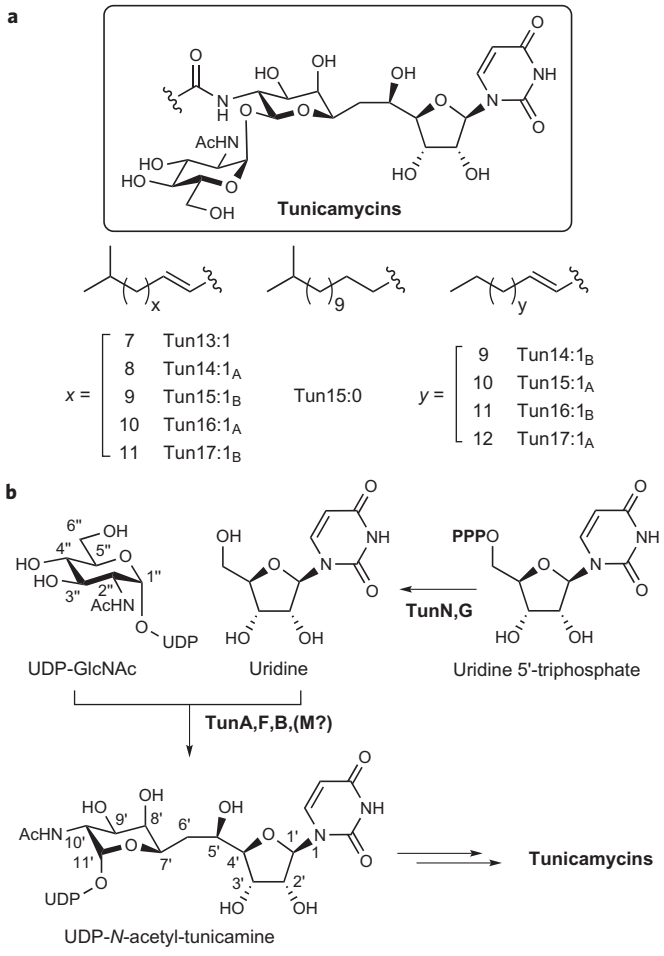


**Figure 1 | Structures of the tunicamycins and early stages of the proposed biosynthetic pathway that creates the 11-carbon chain. a**, Tunicamycin homologues vary in the length, branching and saturation of their fatty acyl side chains. **b**, Proposed biosynthetic pathway of the key intermediate containing the construction of the core tunicamine subunit from primary metabolites uridine 5′-triphosphate (UTP) and UDP-GlcNAc. The creation of suitable intermediates for coupling has no clear precedent in nature. Putative gene products TunA and TunF were previously suggested[24] to participate in its early stages based on analysis of the reported tunicmaycin gene cluster from *S. chartreusis*[24]. The numbering systems used in this manuscript follow carbohydrate nomenclature conventions. For compounds that contain the tunicamine core, the associated 11-carbon chain is indicated by primed atom labels (X′). In areas of the main text where substructures are being discussed, primes have been left out to aid the clarity of the discussion (for example, 4-keto-5,6-ene).

Alignments of TunF with human UDP-glucose-4-epimerase (hGalE) and WbpP and WbgU (Supplementary Fig. S2) revealed that residues 3–35 resemble the $NAD^+$-binding pocket of hGalE[32] and contain the conserved TGxxGxxG signature sequence (6–13)[33]. An $Sx_{24}Yx_3K$ catalytic triad, characteristic of SDR enzymes, is present at positions 115–144 (ref. 33). Ser289 is predicted to act as 'gatekeeper' residue, allowing *N*-acetylated sugar nucleotides into the active site. This is in accord with other UDP-GlcNAc 4-epimerases and hGalE, which accept acetylated substrates and contain unhindered residues at this position. Conversely, it contrasts with *E. coli* GalE (eGalE), which only epimerizes UDP-galactose and has a bulky tyrosine gatekeeper residue[34]. This supports the hypothesis that TunF acts upon an *N*-acetylated sugar.

**TunF is a UDP-GlcNAc 4-epimerase.** To probe TunF function and determine the substrate(s), a codon-optimized *tunF* gene was synthesized and cloned into expression vector pET16b. This was expressed and the protein purified from *E. coli* as an *N*-terminal-$His_{10}$-fusion (Supplementary Fig. S3). The 37.8 kDa protein was incubated with UDP-GlcNAc and conversion was monitored by $^1$H NMR (Supplementary Fig. S4). This revealed the formation of a product with chemical shifts indistinguishable from UDP-GalNAc standard: a decrease in the integration of UDP-GlcNAc-derived peaks mirrored an increase in UDP-GalNAc. In control experiments with heat-denatured TunF, no product was formed. The time course of the reaction (Supplementary Fig. S4) showed the formation of ~30% equilibrium position ($K_{eq} = 0.43$), consistent with related epimerases and reflecting a greater stability of equatorial over axial 4-OH (ref. 35). A high-performance liquid chromatography (HPLC) assay (Supplementary Fig. S5) allowed the determination of kinetic parameters ($K_M = 3.6(\pm 0.2)$ mM and $k_{cat}/K_M = 34.0(\pm 2.8)$ $mM^{-1}$ $min^{-1}$) for TunF towards UDP-GlcNAc.

**TunA is a UDP-GlcNAc 5,6-dehydratase.** The predicted activity of TunA was based on sequence similarity with DesIV and RmlB. Both catalyse oxidation of 4-OH in dTDP-glucose and subsequent E1cB elimination to form α,β-unsaturated-ketone dTDP-4-keto-glucose-5,6-ene[28,29]. In these enzymes, this intermediate undergoes 1,4-conjugate addition of hydride to yield dTDP-6-deoxy-4-keto-glucose (Supplementary Fig. S6).

Codon-optimized *tunA* gene was synthesized and cloned into pET16b. This was expressed and the protein purified from *E. coli* cells as an *N*-terminal-$His_{10}$-fusion (Supplementary Fig. S7). The 37.9 kDa protein product was incubated with putative substrates. Product was only formed from UDP-GlcNAc, rather than the proposed substrate UDP-GalNAc (Supplementary Fig. S8). Surprisingly, the product of TunF was not processed by TunA, and our initial proposals[24] for the order of events during tunicamine biosynthesis were incorrect.

After TunA was incubated with UDP-GlcNAc and $NaBD_4$, mass spectrometry revealed a product compound with $m/z = 589$. The 18-unit reduction in $m/z$ from substrate (UDP-GlcNAc) to product corresponded simply to a dehydrated form. This result and NMR results suggested that no deuterium incorporation/trapping had occurred (Fig. 2). This gave the first suggestion that TunA yields neither the intermediate UDP-4-keto-6-deoxy-GlcNAc-5,6-ene nor the typical dehydrated product UDP-6-deoxy-4-keto-GlcNAc, but instead its allylic alcohol isomer, UDP-6-deoxy-5, 6-ene-GlcNAc.

To distinguish possible dehydration pathways (Fig. 2), the reaction mixture was analysed in detail by $^1$H NMR. UDP-GlcNAc was incubated with TunA in buffered $D_2O$. New resonances from product were distinctly visible: $\delta_H = 5.53$ ppm was assigned to an H-1″ anomeric proton with multiplicity and coupling constants very similar to those of UDP-GlcNAc. Resonances at $\delta_H = 4.85$ ppm were indicative of a 1,1-disubstituted-alkenyl moiety, potentially corresponding to H-6″a,6″b of a terminal alkene and arguing for the formation of a UDP-6-deoxy-GlcNAc-5,6-ene product. This was further supported by the absence of C-6″ methyl group resonance, which would be present if the typical product of dehydratases, UDP-4-keto-6-deoxy-GlcNAc, had been formed. The double-triplet (dt) multiplicity for the resonance at $\delta_H = 4.05$ ppm was assigned to H-4″; critically, this displayed long-range allylic coupling to protons on C-6″ and the $^3J_{4'',3''}$ (9.4 Hz) coupling constant closely matched that of the corresponding H-4″ peak of UDP-GlcNAc; this strongly suggested unchanged stereochemistry at C-4″.

This unusual product of the TunA-catalysed reaction was produced and purified on scale and fully characterized by $^1$H, $^{13}$C, $^{31}$P, correlation spectroscopy (COSY), heteronuclear multiple-quantum correlation (HMQC) and total correlation spectroscopy (TOCSY) NMR experiments and high-resolution mass spectroscopy, and was unambiguously assigned as UDP-6-deoxy-GlcNAc-5,6-ene (Supplementary Figs S9 and S10). To the best of

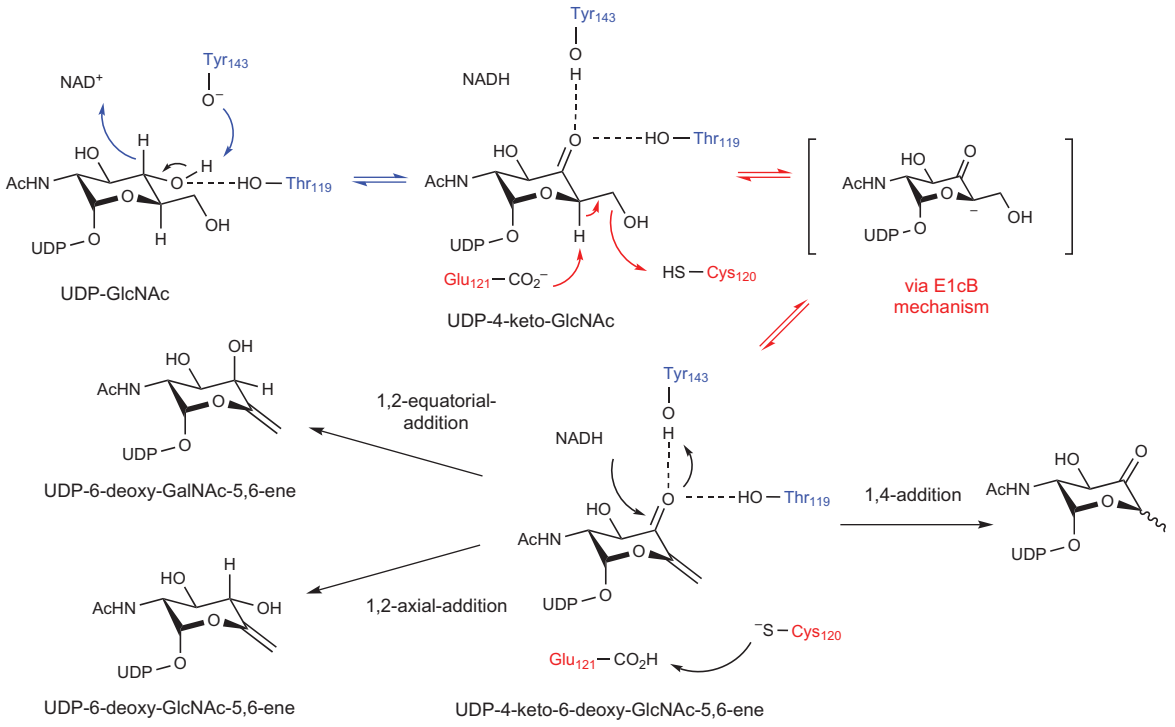


**Figure 2 | Possible TunA-catalysed dehydration pathways for substrate UDP-GlcNAc and putative intermediates.** Initial analysis of the product began with an attempt to 'trap' or react key functional groups that might be expected to be present from typical SDR activity (for example, in either a 4-keto product of 1,4-addition or an α,β-unsaturated keto intermediate). In these cases, sodium borodeuteride ($NaBD_4$, as a source of external nucleophile) would react to introduce a distinctive deuterium label. MS and NMR investigations revealed the formation instead of exo-glycal UDP-6-deoxy-5,6-ene-GlcNAc, which is unreactive to $NaBD_4$.

our knowledge, TunA is the first enzyme to exhibit NDP-sugar-5,6-dehydratase activity, converting 4″, 5″ and 6″ positions of UDP-GlcNAc into an allylic alcohol moiety. This is in stark contrast to all other reported NDP-sugar-4,6-dehydratases that generate NDP-4-keto-6-methyl sugars. HPLC and NMR analyses indicated that TunA catalysed the establishment from UDP-GlcNAc of an equilibrium ($K_{eq} = 0.16$) with $k_{cat} = 0.41(\pm 0.01)\ s^{-1}$ and $K_M = 5.5(\pm 0.3)$ mM (Supplementary Fig. S11).

Insight into the TunA mechanism was gained from other observations. In particular, when the reaction was conducted in buffered $D_2O$, the integration of the H-5″ resonance for starting substrate UDP-GlcNAc was lower in the $^1H$ NMR than for other proton resonances. This reduction suggested partial incorporation of deuterium at C-5″; this site-specific H-5″ ↔ $^2H$-5″ exchange was confirmed by $^2H$ NMR. An additional minor doublet resonance was also observed ($J = 9.1$ Hz) at $\delta_H = 3.52$ ppm, which overlapped with the H-4″ triplet peak of UDP-GlcNAc. This supported the existence of two closely related compounds differing only by the presence of deuterium at C-5″. This partial deuteration implied 'wash out' by deuterated solvent[36] and suggests a rapid, reversible step consistent with an E1cB reaction mechanism, supporting the involvement of a UDP-4-keto-GlcNAc intermediate that is readily deprotonated at C-5″.

**Control of reductive regioselectivity in Tun A.** Given the near identical conservation of key residues in TunA (a 5,6-dehydratase using 1,2-reduction) and, for example, DesIV (a 4,6-dehydratase using 1,4-reduction)[29] suggested by primary sequence alignment (*vide supra*), we sought to determine the mechanism behind this control of regioselectivity (1,2 versus 1,4). TunA was crystallized in the presence of both substrate UDP-GlcNAc and cofactor $NAD^+$ at a pH remote from that of optimal activity to minimize turnover—the resulting X-ray crystal structure was determined to a resolution of 1.9 Å (Supplementary Table S8) as a ternary complex (Fig. 3). The overall structure was superimposed with the ternary complex structures of other dehydratases from the SDR family—dTDP-Glc-4,6-dehydratases DesIV and both RmlBs—with a root-mean-square deviation of 1.3–1.8 Å. The overall structure of TunA can be divided into two domains. The *N*-terminal domain contains the $NAD^+$-binding site and shows the typical Rossmann fold (seven parallel β-strands surrounded by seven α-helices). The smaller *C*-terminal domain binds UDP-GlcNAc and consists of mixed strands of four β-sheets and four α-helices, features also characteristic of the SDR family. The chemistry catalysed by the enzyme occurs at the interface of these domains.

Overall, the interactions of $NAD^+$ and UDP-GlcNAc in their binding sites in TunA are very similar to those at equivalent positions in DesIV and both RmlBs (Fig. 3b and Supplementary Figs S12 and S14). Consistent with the bioinformatics analysis (*vide supra*), mutation of each residue in the TYK motif (to the respective single-point alanine mutants Thr119Ala, Tyr143Ala, Lys147Ala) reduced the enzymatic activity to an undetectable level (Supplementary Table S9). Closer inspection of the site where the GlcNAc moiety and the nicotinamide ring of $NAD^+$ are in close contact, however, reveals some interesting subtleties, which may play important roles in altering the catalytic activity of TunA and hence explain the unique observed reactivity. C-4 of the nicotinamide ring lies 3.4 Å from C-4″ of the GlcNAc ring, a position normally ideal for subsequent hydride transfer[37]. The relative positions of the nicotinamide and hexosamine/hexose ring planes are particularly notable (Fig. 4 and Supplementary Fig. S13). The ribose of $NAD^+$ bearing the nicotinamide group is placed closer to the GlcNAc moiety in the TunA complex than in DesIV/RmlB structures. Moreover, the plane of the nicotinamide ring in TunA is rotated ~20° with respect to the UDP-GlcNAc

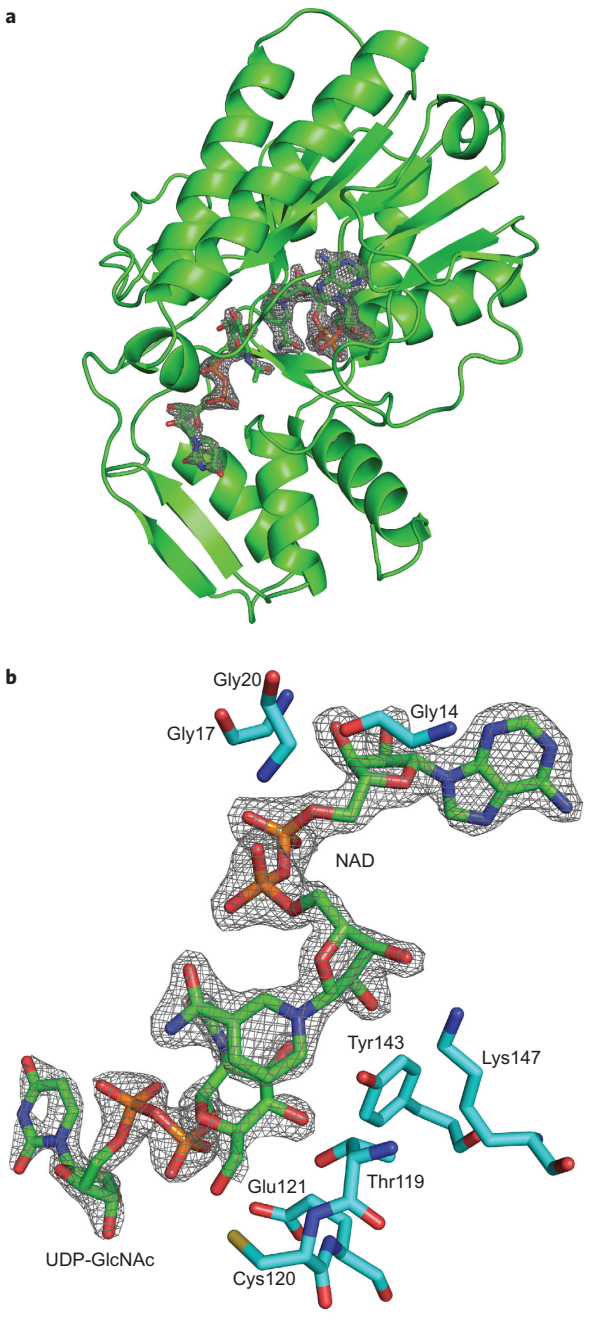


**Figure 3 | Three-dimensional structure of TunA.** The crystal structure contains two TunA molecules per unit cell and each monomer clearly shows a molecule of the substrate bound in the active site together with cofactor $NAD^+$. **a**, Representative model of the TunA monomer showing the observed electron density for the bound UDP-GlcNAc substrate and $NAD^+$ cofactor. **b**, Detailed view of the TunA active site. Electron density maps are $2F_O$–$F_C$ syntheses (grey) contoured at ~1$\sigma$. This figure and Fig. 4a were drawn with PyMOL (http://pymol.sourceforge.net).

ring plane; in the other dehydratases it is approximately parallel to the hexosamines (Fig. 4). The amide carbonyl of the nicotinamide within TunA makes a hydrogen bond to the Val174 backbone amide, thus stabilizing this 'rotated' position (Supplementary Fig. S14); in DesIV/RmlBs the equivalent residue is Asn. This rotation observed only in TunA places C-4 of $NAD^+$/NADH nicotinamide directly above C-4″ of GlcNAc, whereas in DesIV/RmlBs this lies much closer to C-6″ of the substrate sugar. More importantly, the C-4 *si*-face of nicotinamide faces away from C-6″ of GlcNAc in TunA, but maintains a favourable position and angle for hydride delivery at C-4″. This subtle rotation is essentially the sole element controlling the absolute observed switch in 1,2 versus 1,4 reductive regioselectivity (Fig. 2 and Supplementary Fig. S15).

The positions of amino-acid residues probably involved in dehydration across C-5″ and C-6″ are also clearly visible. The most notable Cys120, 2.7 Å from OH-6′, we suggest as a general acid for OH-6″ protonation (Fig. 2). In other dehydratases, Asp at corresponding positions plays this role[28,29]. The adjacent Glu121—conserved across all dehydratases discussed here—is suggested to function as a general base in the abstraction of the H-5″ proton, lying 3.6 Å from C-5″ and with good alignment for axial H-5″. In TunA, Glu121 also forms a 3.1 Å hydrogen bond with OH-6″, an interaction absent from the other dehydratases. Consistent with these suggested critical roles in catalysis, the corresponding single point alanine mutants—Cys120Ala and Glu121Ala—had no detectable enzymatic activities (Supplementary Table S9).

It is notable that the Lys residue hydrogen-bonded to the OH-2″ of dTDP-glucose in the DesIV and RmlBs is replaced by smaller Ala183 in TunA, thus allowing the larger C-2″-acetamido substituent of UDP-GlcNAc. Consistent with this role, the mutation Ala183 → Lys, blocking this acetamide binding site, removed any detectable activity (Supplementary Table S9). In the binding of dTDP-glucose, the DesIV/RmlBs structures show a His residue forming a hydrogen bond to the only hydroxyl (OH-3′) of the substrate 2′-deoxyribose ring. In TunA, Glu267 replaces this residue, forming hydrogen bonds to both OH-2′,3′ of the ribose moiety in UDP-GlcNAc. Interestingly, alteration of Glu267 → Ala gave a single-point mutant that retained some activity, albeit with eightfold reduction in $k_{cat}$ and fivefold increase in $K_M$ (Supplementary Table S9). Notably, the structure determined here indicates that additional hydrogen bonding to OH-2′ provided by the Glu201 side chain may mitigate the associated loss of binding energy to the ribose diol unit during catalysis.

**TunF acts on more than one substrate.** The apparent processing of UDP-GlcNAc as substrate by both TunA and TunF created a conundrum regarding the starting point and ordering of the *tun* pathway (Fig. 5a). Despite the demonstrated UDP-GlcNAc-4-epimerase activity (*vide supra*), TunF could, in principle act upon other substrates (Supplementary Fig. S16).

To investigate this possibility, UDP-GlcNAc was incubated with a mixture of TunF and TunA. Four $^1$H NMR resonances with characteristic multiplicities in the $\delta_H = 5.4$–$5.7$ ppm H-1″ region indicated four distinct species (Fig. 5b). Three corresponded to UDP-GlcNAc, UDP-GalNAc and UDP-6-deoxy-GlcNAc-5,6-ene; the fourth, formed only in the presence of both TunF and TunA, was deduced to be UDP-6-deoxy-GalNAc-5,6-ene (Fig. 5).

To test this hypothesis, a sample of UDP-6-deoxy-GlcNAc-5,6-ene was isolated following incubation of UDP-GlcNAc with 5,6-dehydratase TunA. This alternative substrate was incubated with TunF (Supplementary Fig. S17). As for UDP-GlcNAc as substrate, TunF also catalysed the establishment of an equilibrium ($K_{eq} = 0.43$) from UDP-6-deoxy-GlcNAc-5,6-ene. Notably, the kinetic parameters revealed that UDP-6-deoxy-GlcNAc-5,6-ene is the preferred substrate for TunF ($k_{cat}/K_M = 245(\pm 25)$ versus $34.0(\pm 2.8)$ $mM^{-1}$ $min^{-1}$).

***In vivo* detection of an exo-glycal intermediate.** To assess the relevance of these *in vitro* experiments to tunicamycin biosynthesis *in vivo*, we created an in-frame deletion mutant of *tunB* in which the entire protein-coding sequence was removed. The construction of an in-frame deletion should prevent any polar effects on the expression of downstream genes, while deletion of *tunB* was predicted to lead to the accumulation of

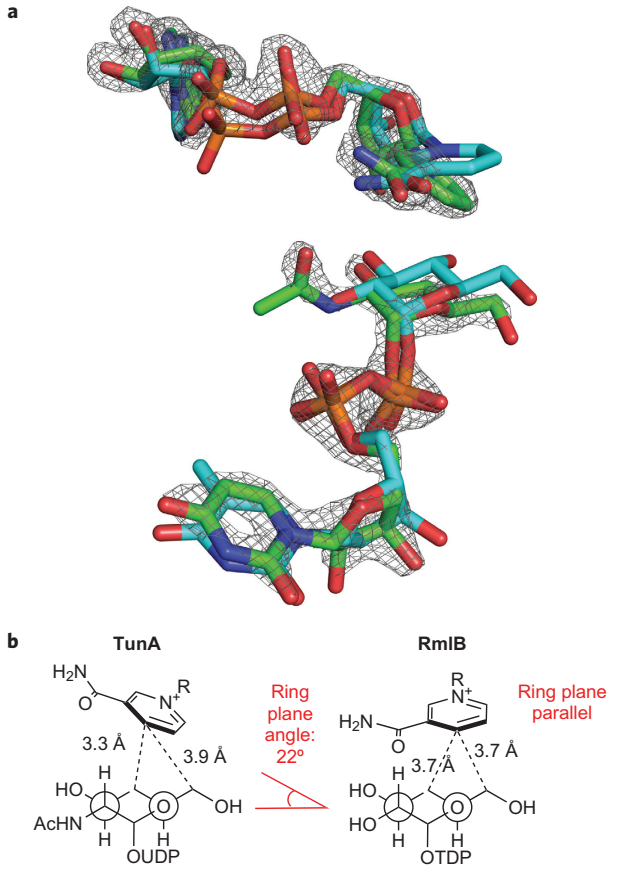


**Figure 4 | Comparison of the conformations of substrates and cofactors in active sites between TunA and RmlB. a**, Colour code for carbon atoms: green, TunA; blue, RmlB. Electron density maps are $2F_O$–$F_C$ syntheses (grey) contoured at ~1$\sigma$; no density data are available for RmlB. **b**, Schematic showing relative positions and angles of substrates and cofactors in active sites of TunA and RmlB. When compared with existing 4,6-dehydratases DesIV/RmlB, the $NAD^+$ nicotinamide and GlcNAc ring planes are no longer parallel and lie ~20° to each other, yet are still positioned to allow efficient hydride-abstraction at C−4″ of UDP-GlcNAc. This subtle rotation plays an important role later in the catalytic cycle, during hydride return to the 4-keto-5,6-ene intermediate. Studies using dTDP-glucose complexed with DesIV have shown that orientation of the plane of α,β-unsaturated intermediate closely mirrors that of the ring plane of the original substrate[29]. If extended to TunA, the altered position and ring plane of nicotinamide in TunA result in poor alignment for hydride return to C-6″ of the intermediate; instead, 1,2-delivery at C-4″ is favoured, followed by re-protonation of O-4″ by Tyr143 (Supplementary Fig. S15). From the determined structure these steps appear able to occur without a need for significant conformational changes.

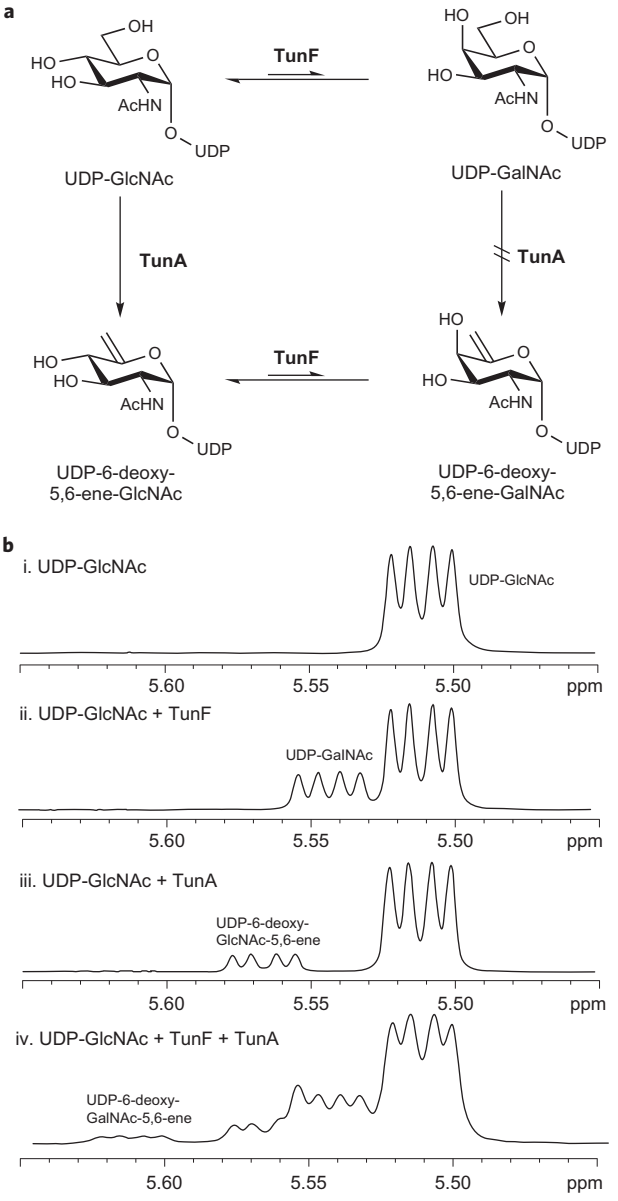


**Figure 5 | Interconversion of UDP-GlcNAc and related biosynthetic intermediates by TunA and TunF. a**, Structures and pathways catalysed by both enzymes together. **b**, NMR evidence of TunA and TunF activity. $^1$H NMR spectra (anomeric H-1″ region) of UDP-GlcNAc incubated with (i) no enzyme, (ii) TunF, (iii) TunA or (iv) TunF and TunA. Because UDP-GalNAc is not a substrate for 5,6-dehydratase TunA, it was deduced that TunF acted upon the product of the TunA reaction, UDP-6-deoxy-GlcNAc-5,6-ene, epimerizing it at C-4″ to form the novel species UDP-6-deoxy-GalNAc-5,6-ene. This was also confirmed by direct incubation of UDP-6-deoxy-GlcNAc-5,6-ene with TunF. UDP-6-deoxy-GlcNAc-5,6-ene is the preferred substrate for TunF; UDP-6-deoxy-GlcNAc-5,6-ene bound more than threefold more tightly than UDP-GlcNAc ($K_M$ = 1.1(±0.1) and 3.6(±0.2) mM, respectively) and $k_{cat}$ values for the exo-glycal substrate were also higher (269(±4) and 122(±3) $min^{-1}$). Note that the strict carbohydrate numbering convention would describe UDP-6-deoxy-GlcNAc-5,6-ene as UDP-6″-deoxy-GlcNAc-5″,6″-ene but the former descriptive notation is used here for clarity in the text.

sufficient exo-glycal for direct observation. This mutational analysis was performed on the cloned tunicamycin biosynthetic gene (*tun*) cluster present in pIJ12003a[24] in the heterologous expression host *Streptomyces coelicolor* M1152. TunB is predicted to catalyse the formation of the C–C bond between C5 of the uridyl moiety and C6 of the central sugar in tunicamycin (see below). If the exo-glycal is the source of this central sugar moiety, then it would be expected to accumulate in a *tunB* mutant. The mutant construct, created by polymerase chain reaction (PCR)-targeting[38], was transferred into *S. coelicolor* M1152[24] by conjugation via tri-parental mating[39]. Successful integration of the mutant construct into the chromosomal φBT1 attachment site was determined by single-colony PCR of kanamycin-resistant exconjugants, yielding *S. coelicolor* M1481.

No tunicamycins were detected from the M1481 culture (Supplementary Fig. S24). However, the nucleotide-rich fraction (Supplementary Fig. S22) contained not only compounds associated with typical metabolism (UDP-HexNAcs ($m/z$ 606 $[M–H]^-$), UDP-hexoses ($m/z$ 565 $[M–H]^-$)), but also compound

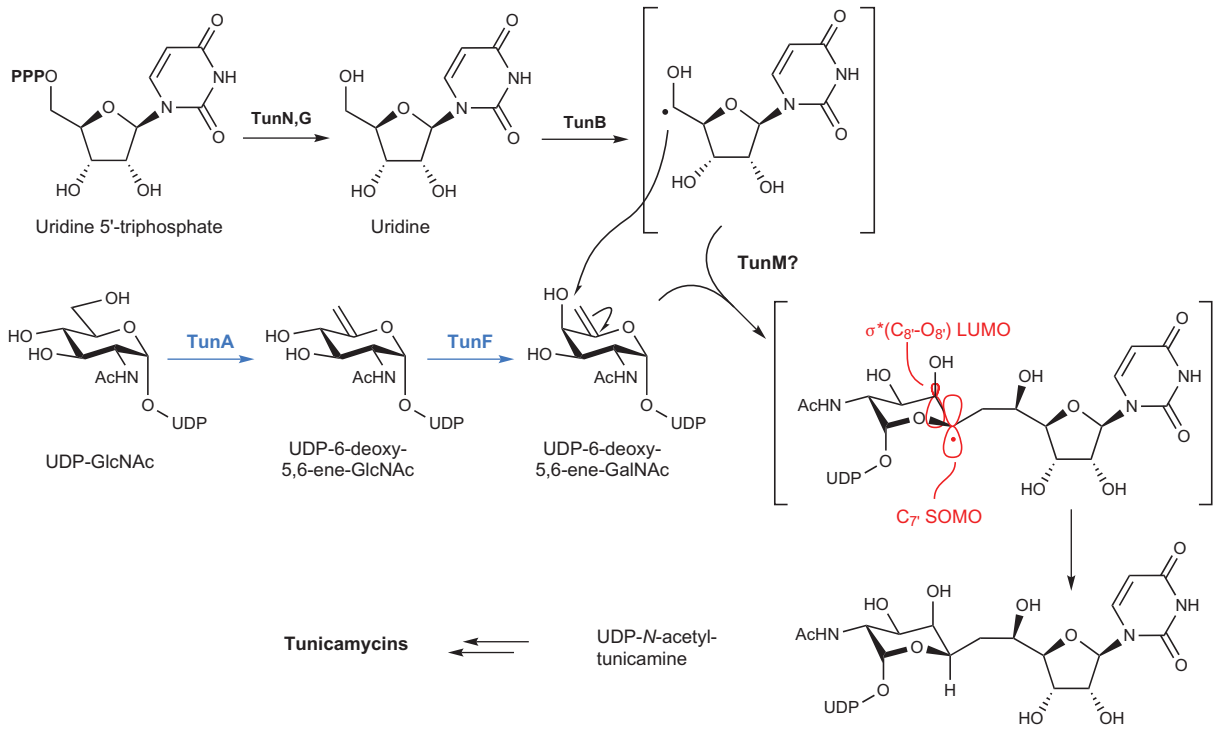


**Figure 6 | Suggested revised biosynthetic pathway to tunicamine, a key precursor of tunicamycin.** Identification of the natural substrates for and functional roles of TunA and TunF have delineated a key portion of the early biosynthetic pathway for the tunicamycins. TunA acts first, forming exo-glycal enol ether UDP-6-deoxy-GlcNAc-5,6-ene from UDP-GlcNAc. TunF then epimerizes this product at C-4″ to yield UDP-6-deoxy-GalNAc-5,6-ene. Together, these enzymes therefore form a unique enol ether intermediate (UDP-6-deoxy-5,6-ene-GalNAc), which has the configuration and constitution to exploit beneficial stereoelectronic interactions (shown in red here in a speculative intermediate) in a suggested subsequent regio- and stereoselective radical addition reaction to generate the correct tunicamine core structure. TunB has been predicted to belong to the radical SAM superfamily, binding *S*-adenosylmethionine (SAM) and a $Fe_4S_4$ redox cluster[24]. It should be noted that the substrate for the TunB-catalysed H-abstraction could also be uridine 5′-monophosphate rather than uridine, as observed in polyoxin and nikkomycin biosynthesis[56,57]. The role of TunM is unclear; it is predicted to belong to the SAM-dependent methyltransferase family[24]. It is possible that it acts as a partner to TunB, mediating the radical process and helping to bring together the $Fe_4S_4$ centre and the two carbohydrate substrates.

corresponding to the predicted exo-glycal ($m/z$ 588 $[M–H]^-$) (Supplementary Fig. S22). Such a disrupted pathway would lead to the accumulation of both exo-glycal epimers. The presence of UDP-6-deoxy-GlcNAc-5,6-ene was confirmed by the addition of an authentic sample (Supplementary Fig. S22). No exo-glycal was detected from *S. coelicolor* M1040 (M1152 harbouring pIJ12003a containing intact *tun* cluster[24]) and the non-producing strain *S. coelicolor* M1037 (M1152 containing only vector[24]) (Supplementary Fig. S23).

## Discussion

The recently reported biosynthetic gene cluster of tunicamycin has allowed the *in vitro* investigation of individual enzymes in the metabolic pathway[24]. TunA and TunF are among those implicated in building its tunicamine core. Here, TunA was found to act as a 5,6-dehydratase, an 'exo-glycal synthase', converting UDP-GlcNAc to exo-glycal UDP-6-deoxy-GlcNAc-5,6-ene; it showed no activity towards UDP-GalNAc. TunF exhibited broad 4-epimerase activity, converting both UDP-GlcNAc and UDP-6-deoxy-GlcNAc-5,6-ene to their respective *galacto*-epimers. Kinetic analysis showed that TunF was sevenfold more active towards the exo-glycal substrate than UDP-GlcNAc; it is an 'exo-glycal epimerase'.

Based on these results, the previously proposed pathway for biosynthesis of the tunicamine core[24] was revised (Fig. 6). TunA acts first on UDP-GlcNAc. TunF then epimerizes its product at C-4″ to yield UDP-6-deoxy-GalNAc-5,6-ene. This raises important implications for the subsequent C–C bond-forming event in the formation of 11-carbon tunicamine. Identification of one of the monosaccharide-derived coupling partners for this key tail-to-tail coupling event as a stable exo-glycal enol ether offers insights into the nature of the uridine-derived coupling partner and the roles of TunB and TunM—enzymes predicted to participate in the coupling process[24]. We suggest that this coupling partner takes the form of a radical, centred at the C-5′ of uridine, in striking contrast to the deduced intermediates of several related nucleoside antibiotics[40–42]. TunB has been predicted to belong to the radical S-adenosyl methionine (SAM) superfamily[24]. Members of this enzyme class catalyse a wide range of radical reactions[43]. We speculate that following H-abstraction from C-5′ of a uridyl moiety, radical addition to the terminal carbon of the exo-glycal coupling partner would give an undecose radical intermediate stabilized by several key interactions (Fig. 6)[44]. An exo-glycal with an axial OH-8′ (such as that formed by the sequential action of TunA and then TunF) creates important consequent stabilizing interactions (C7′-SOMO with C8′–O8′-$\sigma$*-LUMO)[44]. Similar radicals perform selective axial H-abstraction by virtue of quasi-homo-anomeric effects[44,45], which here would lead to the stereochemistry required for tunicamine. This effect has been previously exploited in the stereoselective synthesis of β-*O*-[46] and *C*-[47] glycosides. Moreover, the addition of radicals to exo-glycal acceptors has a synthetic precedent[48,49], not least in Gin and Myer's chemical synthesis of tunicamycin[21], which we reveal here may, at least in this aspect, be biomimetic. Importantly, the products of *S. coelicolor* strains (with/without *tun* cluster; with/without *tunB* mutation) are consistent with this revised pathway and the intermediacy of exo-glycals. Detection of exo-glycal only from *S. coelicolor* M1481, which contains the *tun* gene cluster but with *tunB* deleted, suggests

that exo-glycals are formed only transiently and at low levels in uninterrupted biosynthesis and not at all in cells that do not produce tunicamycin. The loss of tunicamycin production caused by *tunB* deletion also confirms its essential role.

The structure of TunA is similar to those of others from the SDR family but differs critically in active site arrangement. Indeed, we suggest that this unique 5,6-dehydratase shares the same first steps of other SDRs (Supplementary Fig. S6), deviating only at the α,β-unsaturated-keto intermediate. 1,2-Hydride delivery, observed in TunA for the first time, forms a 5,6-ene product and contrasts with the 1,4-regioselectivity observed thus far in the SDRs (Fig. 2). The major source of this altered regioselectivity is attributed to subtle changes in the relative positions of the $NAD^+$ cofactor and UDP-GlcNAc substrate within the TunA active site (Fig. 3).

TunA contains an active-site Cys that is absent from other SDR enzymes. Within the 4,6-dehydratases DesIV/RmlB, a conserved Asp/Glu diad is involved in dehydration across C-5″/C-6″. At equivalent positions in TunA, Glu121 is retained while Cys120 lies in place of Asp, and mutation of either abolishes activity. Although expected to act as a general acid like aspartic acid, it is possible that the higher $pK_a$ of cysteine may prevent unwanted protonation (which might be catalysed by an Asp were this to be found at position 120) of the unique enol ether product formed by TunA, thus protecting it from unwanted hydrolysis in the enzyme active site. Cys120 may also provide more favourable hydrophobic interactions with the C=C double bond that is uniquely formed here.

Together, the TunA and TunF enzymes have revealed not only new modes of biosynthesis used in the assembly of the unique 11-carbon chain that makes up the core of tunicamycin, they have also given insight into surprising biological intermediates (exo-glycals) and the mechanistic subtlety behind modes of biocatalytic selectivity (1,2 versus 1,4 reduction) that are used for their formation. Remarkably, this discovery of a new pathway, which we suggest exploits the enol ether moiety of these exo-glycals, until now had no biological precedent but does have chemical synthetic precedent[21]. TunA and TunF may act together to deliver a substrate for radical coupling that is chemically logical in ensuring both regioselecivity and stereoselectivity (Fig. 5). It therefore presents, to our knowledge, a rare example of the *post hoc* validation of a chemical synthetic strategy[21] as being biomimetic.

## Methods

**Chemicals, enzymes and bacterial strains.** Unless otherwise stated, chemical reagents were purchased from Sigma-Aldrich, media components from Sigma-Aldrich or Melford Laboratories and enzymes from Sigma-Aldrich or Invitrogen. Media and general methods for the growth and propagation of *E. coli* were as described in ref. 50.

**Cloning and expression of *tunA* and *tunF*.** The gene sequences of *tunA* and *tunF* from *S. chartreusis* NRRL 3882 (Genbank accession HQ172897) were codon optimized for *E. coli* and synthesized by GenScript USA. The genes, both supplied in vector pET16b (Novagen), were introduced into *E. coli* BL21(DE3) by transformation and expressed using standard procedures (Supplementary Methods). Protein purification after cell harvest was performed using immobilized metal affinity chromatography according to standard methods (Supplementary Methods).

**HPLC activity assay.** UDP-GlcNAc 4,6-dehydratase activity was typically assayed with a reaction mixture volume of 100 μl, incubated at 30 °C for 20 min, and containing 5 mM UDP-GlcNAc (or UDP-GalNAc) with or without 2 mM $NAD^+$ in 50 mM Tris, pH 7.5, and with an appropriate amount of the enzyme extract. For the trapping experiments, 25 mM sodium borodeuteride was added to the mixture and incubated at 22 °C for an additional 10 min. Control reactions lacking particular components were carried out to determine their necessity for enzymatic conversion. The reaction mixtures were analysed by HPLC (Supplementary Methods).

**HPLC time course assay.** UDP-GlcNAc (5 mM) was prepared in 0.05 M Tris buffer, pH 7.5, with or without 5 mM $MgCl_2$. TunA was added to a final concentration of 0.12 mg $ml^{-1}$. The reaction was mixed by vortexing and incubated at 30 °C. Small aliquots were withdrawn at a range of time intervals, filtered through viva spin (Sartorius, 10K NMWCO) and analysed by HPLC (Supplementary Methods). Substrate and product peaks eluted at 18 and 19 min, respectively. These were integrated and a time course of TunA activity plotted (Supplementary Fig. S11).

**HPLC kinetic assay.** Appropriate concentrations of UDP-GlcNAc were prepared in 0.05 M Tris buffer, pH 7.5, containing 5 mM $MgCl_2$. TunA was added to a final concentration of 0.12 mg $ml^{-1}$. The reaction was mixed by vortexing and incubated at 30 °C. Each reaction was stopped after 5 min by flash freezing in liquid nitrogen. Each sample was then boiled for 1 min, filtered through viva spin (Sartorius, 10K NMWCO) and analysed by HPLC (Supplementary Methods). Substrate and product peaks eluted at 26 and 29 min, respectively. From the integration of these peaks a Michaelis–Menten curve of TunA activity was constructed (Supplementary Fig. S11).

**NMR activity assay.** Enzymatic reactions were performed in 25 mM Tris, pH 8.0, with 25–100 μg of freshly purified TunA and 77 mM UDP-GlcNAc in a total reaction volume of 300 μl. After incubation for 1 h at 37 °C, the mixture was flash frozen and lyophilized. The resulting residue was dissolved in $D_2O$ (600 μl) and analysed by NMR. As control experiments, the same procedures were applied to samples lacking either TunA enzyme or UDP-GlcNAc. For isolation and full characterization of the UDP-6-deoxy-GlcNAc-5,6-ene product see Supplementary Methods and Supplementary Figs S8, S9 and S10.

**Functional and kinetic assay of TunF.** The activity of TunF was measured in a similar way to that of TunA. See Supplementary Methods for details.

**TunA crystallization and structure solution.** The cubic-shaped crystals of TunA protein, typically 115 × 115 μm and belonging to space group *P*1 ($a = 45.5$, $b = 51.1$, $c = 67.8$(Å), $\alpha = 98.13$, $\beta = 106.65$, $\gamma = 94.36$ (°), two molecules per asymmetric unit), were obtained after six days at 20 °C using a hanging drop method with 20 mg $ml^{-1}$ protein, 20 mM Tris-HCL (pH 7.8) and 2 mM UDP-GlcNAc in the protein solution, and 20% polyethylene glycol 3350, 100 mM 8 v/v tacsimate (pH 6) in the reservoir solution. A 1.8 Å data set was collected from a single crystal using a Rigaku Saturn 944+ charge-coupled device detector and FRE+ SuperBright X-ray generator equipped with a copper anode at 100 K. The X-ray data were processed with HKL2000 and scaled with SCALEPACK[51]. The structure was solved by molecular replacement using an alanine model constructed from the structure of dTDP-glucose 4,6-dehydratase (PDB ID 1R66)[29]. Successive initial model building was carried out using the Phenix program (v1.6)[52] and subsequent model building/rebuilding were performed in COOT[53,54]. Model refinement was performed with Refmac in the CCP4 program suite, by setting aside 5% of the observed reflection data for cross-validation. The structure was refined to a resolution of 1.9 Å. The final model has an *R* factor of 18.5% and an $R_{free}$ of 23.3%. Relevant X-ray data collection and structure solution statistics are presented in Supplementary Table S8. Data are deposited with the code PDB ID code 3VPS.

**Construction of the *tunB* deletion mutant.** *S. coelicolor* M1481 (M1152 carrying the *tunB*-deleted construct pIJ12541 integrated at the chromosomal φBT1 attachment (*att*) site) was made by first replacing *tunB* in pIJ12003a[24] with an apramycin resistance gene using PCR-targeting[38] with the pIJ773 apramycin cassette amplified with primers tunB20 (CTTCCAAGAGGAGGGGGCCGACTGATGA CCGGCTACACCATTCCGGGGATCCGTCGACC) and tunB19 (GGCCTCC CTGGACAAGGCCTACCTCACCTCCGCGCCTTCTGTAGGCTGGAGCTGC TTC). Correct targeting was confirmed by PCR using primers tunBtstF (TCGCGACTTCACCTACATCA) and tunBtstR (TGAGGTCGTACAGGCG TATG). The apramycin resistance cassette was then removed by site-specific recombination using FLP-recombinase[38] generating pIJ12541. This construct was introduced in *S. coelicolor* M1152 by conjugation[38] to yield *S. coelicolor* M1481. Correct integration of pIJ12541 at the chromosomal φBT1 *att* site was confirmed by PCR using primer pairs BT1V1(GGTGCGAATAA GGGACAGTG) plus BT1C1 (CACGAGCGGAAACGTACC), and BT1C2 (GTACCAGTTGGCCGTCACC) plus BT1V2 (ACGTCCACGAACTCACCTG).

**Construction of *S. coelicolor* M1037.** pRT802[55] was introduced into *S. coelicolor* M1152 by conjugation, generating *S. coelicolor* M1037. pRT802 integrates at the chromosomal φBT1 *att* site.

**Construction of *S. coelicolor* M1040.** pIJ12003a, a pRT802 derivate containing the minimal tunicamycin gene cluster[24], was introduced into *S. coelicolor* M1152 by conjugation, generating strain *S. coelicolor* M1040.

Received 28 June 2011; accepted 3 April 2012; published online 20 May 2012

## References

1. Brandish, P. E. *et al.* Modes of action of tunicamycin, liposidomycin B, and mureidomycin A: inhibition of phospho-*N*-acetylmuramyl-pentapeptide translocase from *Escherichia coli*. *Antimicrob. Agents Chemother.* **40,** 1640–1644 (1996).
2. Heifetz, A., Keenan, R. W. & Elbein, A. D. Mechanism of action of tunicamycin on the UDP-GlcNAc:dolichyl-phosphate GlcNAc-1-phosphate transferase. *Biochemistry* **18,** 2186–2192 (1979).
3. Tamura, G. *Tunicamycin* (Japan Scientific Societies Press, 1982).
4. Hamill, R. L., Hoehn, M. H. & Boeck, L. D. Process for preparing tunicamycin. US patent 4,336,333 (1980).

5. Takatsuki, A., Arima, K. & Tamura, G. Tunicamycin, a new antibiotic: 1. Isolation and characterization of tunicamycin. *J. Antibiot.* **24,** 215–223 (1971).
6. Takatsuki, A. *et al.* Structural elucidation of tunicamycin: 2. Structure of tunicamycin. *Agric. Biol. Chem.* **41,** 2307–2309 (1977).
7. Tsvetanova, B. C. & Price, N. P. J. Liquid chromatography-electrospray mass spectrometry of tunicamycin-type antibiotics. *Anal. Biochem.* **289,** 147–156 (2001).
8. Thrum, H. *et al.* Streptovirudins, new antibiotics with antibacterial and antiviral activity: 1. Culture taxonomy, fermentation and production of streptovirudin complex. *J. Antibiot.* **28,** 514–521 (1975).
9. Vogel, P. *et al.* Isolation of a group of glycolipid toxins from seedheads of annual ryegrass (*Lolium rigidum* Gaud.) infected by *Corynebacterium rathayi*. *Austr. J. Exp. Biol. Med. Sci.* **59,** 455–467 (1981).
10. Kenig, M. & Reading, C. Holomycin and an antibiotic (MM 19290) related to tunicamycin, metabolites of *Streptomyces clavuligerus*. *J. Antibiot.* **32,** 549–554 (1979).
11. Nakamura, S., Arai, M., Karasawa, K. & Yonehara, H. On an antibiotic, mycospocidin. *J. Antibiot.* **10,** 248–253 (1957).
12. Mizuno, M., Shimojima, Y., Sugawara, T. & Takeda, I. Antibiotic 24010. *J. Antibiot.* **24,** 896–899 (1971).
13. Tamura, G., Sasaki, T., Matsuhashi, M., Takatsuki, A. & Yamasaki, M. Tunicamycin inhibits formation of lipid intermediate in cell-free peptidoglycan synthesis of bacteria. *Agric. Biol. Chem.* **40,** 447–449 (1976).
14. Walsh, C. Where will new antibiotics come from? *Nature Rev. Microbiol.* **1,** 65–70 (2003).
15. Xu, L., Appell, M., Kennedy, S., Momany Frank, A. & Price Neil, P. J. Conformational analysis of chirally deuterated tunicamycin as an active site probe of UDP-*N*-acetylhexosamine:polyprenol-P *N*-acetylhexosamine-1-P translocases. *Biochemistry* **43,** 13248–13255 (2004).
16. Elbein, A. D. The tunicamycins — useful tools for studies on glycoproteins. *Trends Biochem. Sci.* **6,** 219–221 (1981).
17. Danishefsky, S. J., Deninno, S. L., Chen, S., Boisvert, L. & Barbachyn, M. Fully synthetic stereoselective routes to the differentially protected subunits of the tunicamycins. *J. Am. Chem. Soc.* **111,** 5810–5818 (1989).
18. Ichikawa, S. & Matsuda, A. Synthesis of tunicaminyluracil derivatives. *Nucleosides Nucleotides Nucleic Acids* **23,** 239–253 (2004).
19. Karpiesiuk, W. & Banaszek, A. Stereoselective syntheses of the *O,N*-protected subunits of the tunicamycins. *Carbohydr. Res.* **299,** 245–252 (1997).
20. Ramza, J. & Zamojski, A. New convenient synthesis of tunicamine. *Tetrahedron* **48,** 6123–6134 (1992).
21. Myers, A. G., Gin, D. Y. & Rogers, D. H. Synthetic studies of the tunicamycin antibiotics. Preparation of (+)-tunicaminyluracil, (+)-tunicamycin-V, and 5′-*epi*-Tunicamycin-V. *J. Am. Chem. Soc.* **116,** 4697–4718 (1994).
22. Suami, T., Sasai, H., Matsuno, K. & Suzuki, N. Synthetic approaches toward antibiotic tunicamycins. Part VIII. Total synthesis of tunicamycin. *Carbohydr. Res.* **143,** 85–96 (1985).
23. Tsvetanova, B. C., Kiemle, D. J. & Price, N. P. J. Biosynthesis of tunicamycin and metabolic origin of the 11-carbon dialdose sugar, tunicamine. *J. Biol. Chem.* **277,** 35289–35296 (2002).
24. Wyszynski, F. J., Hesketh, A. R., Bibb, M. J. & Davis, B. G. Dissecting tunicamycin biosynthesis by genome mining: cloning and heterologous expression of a minimal gene cluster. *Chem. Sci.* **1,** 581–589 (2010).
25. Chen, W. *et al.* Characterization of the tunicamycin gene cluster unveiling unique steps involved in its biosynthesis. *Prot. Cell* **1,** 1093–1105 (2010).
26. Karki, S., Kwon, S-Y. & Kwon, H-J. Cloning of tunicamycin biosynthetic gene cluster from *Streptomyces chartreusis* NRRL 3882. *J. Kor. Soc. Appl. Biol. Chem.* **54,** 136–140 (2011).
27. Berman, H., Henrick, K. & Nakamura, H. Announcing the worldwide Protein Data Bank. *Nature Struct. Biol.* **10,** 980–980 (2003).
28. Allard, S. T. M. *et al.* Toward a structural understanding of the dehydratase mechanism. *Structure* **10,** 81–92 (2002).
29. Allard, S. T. M., Cleland, W. W. & Holden, H. M. High resolution X-ray structure of dTDP-glucose 4,6-dehydratase from *Streptomyces venezuelae*. *J. Biol. Chem.* **279,** 2211–2220 (2004).
30. Demendi, M., Ishiyama, N., Lam, J. S., Berghuis, A. M. & Creuzenet, C. Towards a better understanding of the substrate specificity of the UDP-*N*-acetylglucosamine C4 epimerase WbpP. *Biochem. J.* **389,** 173–180 (2005).
31. Kowal, P. & Wang, P. G. New UDP-GlcNAc C4 epimerase involved in the biosynthesis of 2-acetamino-2-deoxy-L-altruronic acid in the *O*-antigen repeating units of *Plesiomonas shigelloides* O17. *Biochemistry* **41,** 15410–15414 (2002).
32. Jornvall, H. *et al.* Short-chain dehydrogenases reductases (SDR). *Biochemistry* **34,** 6003–6013 (1995).
33. Filling, C. *et al.* Critical residues for structure and catalysis in short-chain dehydrogenases/reductases. *J. Biol. Chem.* **277,** 25677–25684 (2002).
34. Schulz, J. M. *et al.* Determinants of function and substrate specificity in human UDP-galactose 4′-epimerase. *J. Biol. Chem.* **279,** 32796–32803 (2004).
35. Creuzenet, C., Belanger, M., Wakarchuk, W. W. & Lam, J. S. Expression, purifcation, and biochemical characterization of WbpP, a new UDP-GlcNAc C4 epimerase from *Pseudomonas aeruginosa* serotype O6. *J. Biol. Chem.* **275,** 19060–19067 (2000).
36. Gross, J. W., Hegeman, A. D., Vestling, M. M. & Frey, P. A. Characterization of enzymatic processes by rapid mix-quench mass spectrometry: the case of dTDP-glucose 4,6-dehydratase. *Biochemistry* **39,** 13633–13640 (2000).
37. Allard, S. T. M. *et al.* The crystal structure of dTDP-D-glucose 4,6-dehydratase (RmlB) from *Salmonella enterica* serovar Typhimurium, the second enzyme in the dTDP-L-rhamnose pathway. *J. Mol. Biol.* **307,** 283–295 (2001).
38. Gust, B. *et al.* Lambda red-mediated genetic manipulation of antibiotic-producing *Streptomyces*. *Adv. Appl. Microbiol.* **54,** 107–128 (2004).
39. Kieser, T., Bibb, M. J., Buttner, M. J., Chater, K. F. & Hopwood, D. A. *Practical Streptomyces Genetics* (The John Innes Foundation, 2000).
40. Kaysser, L. *et al.* Identification and manipulation of the caprazamycin gene cluster lead to new simplified liponucleoside antibiotics and give insights into the biosynthetic pathway. *J. Biol. Chem.* **284,** 14987–14996 (2009).
41. Kaysser, L., Siebenberg, S., Kammerer, B. & Gust, B. Analysis of the liposidomycin gene cluster leads to the identification of new caprazamycin derivatives. *ChemBioChem* **11,** 191–196 (2010).
42. Rackham, E. J., Gruschow, S., Ragab, A. E., Dickens, S. & Goss, R. J. M. Pacidamycin biosynthesis: identification and heterologous expression of the first uridyl peptide antibiotic gene cluster. *ChemBioChem* **11,** 1700–1709 (2010).
43. Marsh, E. N. G., Patterson, D. P. & Li, L. Adenosyl radical: reagent and catalyst in enzyme reactions. *ChemBioChem* **11,** 604–621 (2010).
44. Giese, B. The stereoselectivity of intermolecular free radical reactions. *Angew. Chem. Int. Ed. Engl.* **28,** 969–980 (1989).
45. Giese, B. & Dupuis, J. Anomeric effect of radicals. *Tetrahedron Lett.* **25,** 1349–1352 (1984).
46. Kahne, D., Yang, D., Lim, J. J., Miller, R. & Paguaga, E. The use of alkoxy-substituted anomeric radicals for the construction of beta-glycosides. *J. Am. Chem. Soc.* **110,** 8716–8717 (1988).
47. Crich, D. & Lim, L. B. L. Synthesis of 2-deoxy-β-C-pyranosides by diastereoselective hydrogen-atom transfer. *Tetrahedron Lett.* **31,** 1897–1900 (1990).
48. Cipolla, L., Liguori, L., Nicotra, F., Torri, G. & Vismara, E. Glycomimetics via a new glycoexoenitols-malonyl radical C–C bond formation. *Chem. Commun.* 1253–1254 (1996).
49. Vauzeilles, B. & Sinay, P. Selective radical synthesis of β-C-disaccharides. *Tetrahedron Lett.* **42,** 7269–7272 (2001).
50. Sambrook, J. & Russell, D. *Molecular Cloning: A Laboratory Manual* (Cold Spring Harbor Laboratory Press, 2000).
51. Otwinowski, Z. & Minor, W. Processing of X-ray diffraction data collected in oscillation mode. *Methods Enzymol.* **276,** 307–326 (1997).
52. Adams, P. D. *et al.* PHENIX: a comprehensive Python-based system for macromolecular structure solution. *Acta Crystallogr. D* **66,** 213–221 (2010).
53. Emsley, P. & Cowtan, K. COOT: model-building tools for molecular graphics. *Acta Crystallogr. D* **60,** 2126–2132 (2004).
54. Emsley, P., Lohkamp, B., Scott, W. G. & Cowtan, K. Features and development of COOT. *Acta Crystallogr. D* **66,** 486–501 (2010).
55. Gregory, M. A., Till, R. & Smith, M. C. M. Integration site for Streptomyces phage BT1 and development of site-specific integrating vectors. *J. Bacteriol.* **185,** 5320–5323 (2003).
56. Chen, W. *et al.* Characterization of the polyoxin biosynthetic gene cluster from *Streptomyces cacaoi* and engineered production of polyoxin H. *J. Biol. Chem.* **284,** 10627–10638 (2009).
57. Ginj, C., Ruegger, H., Amrhein, N. & Macheroux, P. 3′-Enolpyruvyl-UMP, a novel and unexpected metabolite in nikkomycin biosynthesis. *ChemBioChem* **6,** 1974–1976 (2005).


## Acknowledgements

The authors gratefully acknowledge B. Odell (Oxford University) for help with the NMR experiments. This work was supported by the EPSRC (DTA studentship for F.J.W.), the Bill and Melinda Gates Foundation (S.S.L.) and BBSRC (J.P.G-E. and M.J.B). G.J.D and B.G.D. are Royal Society Wolfson Research Merit Award recipients. This manuscript is dedicated to the memory of Professor David Gin.

## Author contributions

F.J.W. cloned *tunF*, purified the protein and performed functional and kinetic analyses of TunF. S.S.L. and T.Y. cloned *tunA* and its mutants, purified the resulting proteins and performed functional analyses. S.S.L. performed the kinetic analyses. TunA was crystallized by T.Y. The 3D structure was determined by S.J.L., and S.S.L., B.G.D and G.J.D. carried out its analysis. H.W. and J.P.G-E. created the *tunB* mutant strain and extracts. M.J.B. designed the deletion strategy. H.W., M.J.B. and B.G.D. analysed the extracts. The manuscript was written by F.J.W., S.S.L., M.J.B., G.J.D. and B.G.D.

## Additional information

The authors declare competing financial interests: details accompany the full-text HTML version of the paper at www.nature.com/naturechemistry. Supplementary information accompanies this paper at www.nature.com/naturechemistry. Reprints and permission information is available online at http://www.nature.com/reprints. Correspondence and requests for materials should be addressed to B.G.D.